HYDROLOGICAL PROCESSES
Hydrol. Process. **14**, 1523–1536 (2000)

Clay aquitards as isotopic archives of Holocene palaeoclimate in the Northern Great Plains: sensitivity analysis

S. J. Birks,[1]* V. H. Remenda[2] and T. W. D. Edwards[1,3]

[1] *Department of Earth Sciences, University of Waterloo, Waterloo ON N2L 3G1, Canada*
[2] *Department of Geological Sciences, Queen's University, Kingston ON K7L 3N6, Canada*
[3] *GSF-Institut fur Hydrologie, Ingolstadter Landstraße 1, 85764 Neuherberg, Germany*

Abstract:

The vertical distributions of ^{18}O and ^{2}H in porewater of a glaciolacustrine clay were simulated to explore the potential conservation of signals deriving from changes in the isotopic composition of Holocene precipitation in low-permeability deposits. The simulations used a groundwater velocity of zero, assuming that transport was solely by diffusion. As expected, distributions were highly sensitive to the timing of Holocene events, with recent events having the greatest preservation potential. Simulations show that these signals are confined to the area immediately below the weathered zone, where infiltration of modern water via fractures or fluctuations in the water table could threaten signal preservation in the field. Century-scale events with magnitudes of 6‰ or less in $\delta^{18}O$ have little effect on the isotopic profiles if they occur more than 1000 years ago. Longer duration events occurring more than 1000 years ago are preserved as slight alterations in the shape of the isotopic profiles.

Differences in the effective diffusion coefficients for $^{1}H^{2}H^{16}O$ and $^{1}H_2{}^{18}O$ result in alteration of the original *d*-excess ($d = \delta^2H - 8\delta^{18}O$). Hence this parameter is not conservative in groundwater environments where transport is dominantly by diffusion. On the other hand, simulated vertical profiles of *d*-excess amplify fluctuations in the isotopic composition of precipitation that are subdued in the individual profiles of $\delta^{18}O$ and δ^2H.

Simulations that include Holocene events with timings, durations and magnitudes estimated for the Hypsithermal, Medieval Warm Period and Little Ice Age result in distributions that differ from the baseline by $\approx$0·6‰ in $\delta^{18}O$ ($\approx$5‰ in δ^2H). That these events are preserved as a measurable offset in the isotopic profile suggests that some aquitards can be used to reconstruct or constrain mid to late Holocene palaeoprecipitation. The small magnitude of these positive offsets suggest that exclusion of Holocene events in the input functions used to constrain parameters by fitting measured isotopic profiles with simulated diffusion profiles, probably has a minimal effect on the parameters they are used to estimate, but could result in a slight overestimation of parameters such as velocity or time since deglaciation. Copyright © 2000 John Wiley & Sons, Ltd.

KEY WORDS aquitard porewaters; stable isotopes; *d*-excess; diffusion; palaeoprecipitation

INTRODUCTION

Few archives of the stable isotope content of past precipitation are available in the northern Great Plains of North America. In some hydrogeological settings, glaciolacustrine clay aquitards may preserve connate waters at depth that retain a depleted isotopic signature deriving from late-glacial precipitation, despite progressive overprinting by downward diffusion of water molecules containing ^{18}O and ^{2}H from more recent, isotopically enriched precipitation. Connate waters are best preserved in thick, unfractured, sequences of

* Correspondence to: S. J. Birks, Department of Earth Sciences, University of Waterloo, Waterloo ON N2L 3G1 Canada. E-mail: sjbirks@sciborg.uwaterloo.ca

Received September 1997
Accepted 14 June 1999

clayey sediment having small hydraulic gradients. The large glacial–interglacial shifts in $\delta^{18}O$ and $\delta^{2}H$ values (respectively *c*. 10 and 80‰) have been detected at a number of sites in stratigraphic profiles of the porewaters of Glacial Lake Agassiz deposits (Remenda *et al*., 1994) and potential may exist to resolve some features of the finer structure as a source of information about more recent fluctuations in the isotopic composition of post-glacial precipitation.

The present investigations were undertaken to simulate how isotopic signals possibly associated with Holocene climatic variations might be preserved in the diffusive porewater regime of Lake Agassiz clay. In addition to evaluating the potential use of aquitard porewater as an isotopic archive of palaeoclimate, this sensitivity analysis also provides important insight about the robustness of hydraulic parameters inferred using different isotopic input functions.

The input function commonly used in the simulation of $\delta^{18}O$ and $\delta^{2}H$ profiles in clay aquitards in glaciated areas of North America is based on a simplified approximation of the $\delta^{18}O$ and $\delta^{2}H$ of polar precipitation recorded in the Greenland ice core (GRIP members, 1993; Grootes *et al*., 1993) and consists of an instantaneous change from glacial to modern precipitation isotope contents at 10 000 yr ago (Figure 1). This

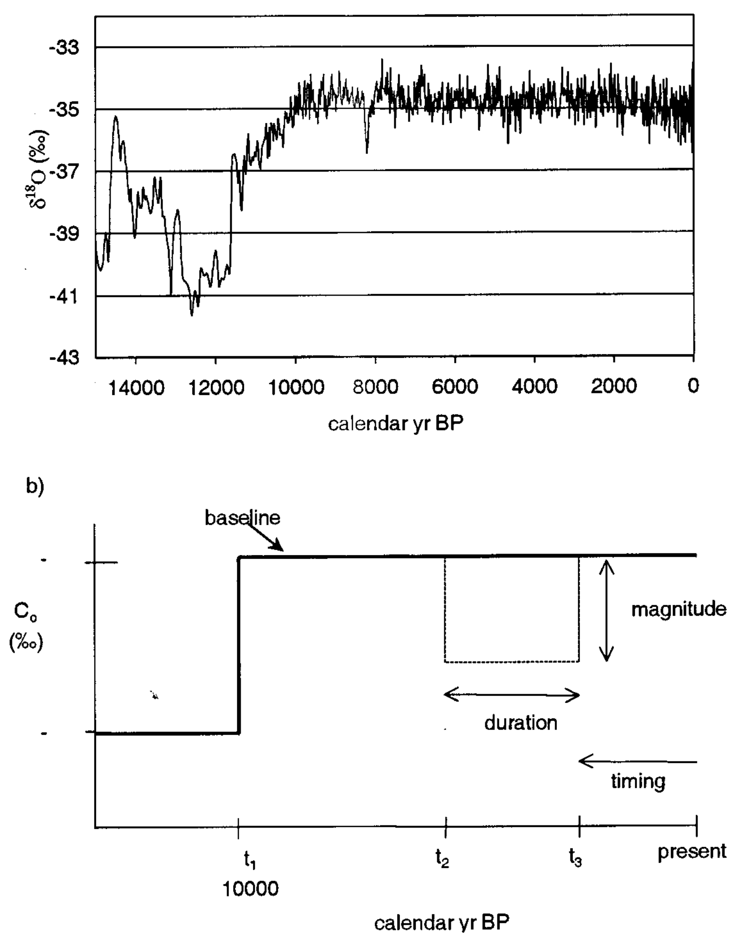

Figure 1. (a) $\delta^{18}O$ record from the GISP2 ice-core, Greenland (after Grootes *et al*., 1993). (b) Schematic of the 'baseline' input function (solid line) that assumes an instantaneous change in the stable isotope composition of precipitation occurring 10 000 calendar years BP and a constant stable isotope content for precipitation over the Holocene. Dotted lines show how the input function was altered. Values for timings, durations (t_2 and t_3) and magnitudes are given in Table I

Table I. Summary of the input functions presented in this paper. Each input function consists of the baseline function with a Holocene 'event' with different timings, durations and magnitudes. The C_0 concentrations listed here refer to $\delta^{18}O$. However, each simulation was repeated using a C_0 value for $\delta^{2}H$ calculated so that the waters would plot on the GMWL

Simulation	Timing (years BP)	Duration (years)	Magnitude (‰)	t_1 (years BP)	C_0 (t_1) (‰)	t_2 (years BP)	C_0 (t_2) (‰)	t_3 (years BP)	C_0 (t_3) (‰)
Baseline	—	—	—	10 000	−15	—	—	—	—
1	100	100	3	10 000	−15	200	−18	100	−15
2	100	100	6	10 000	−15	200	−21	100	−15
3	100	1000	3	10 000	−15	1100	−18	100	−15
4	100	1000	6	10 000	−15	1100	−21	100	−15
5	100	4000	3	10 000	−15	4100	−18	100	−15
6	100	4000	6	10 000	−15	4100	−21	100	−15
7	1000	100	3	10 000	−15	1100	−18	1000	−15
8	1000	100	6	10 000	−15	1100	−21	1000	−15
9	1000	1000	3	10 000	−15	2000	−18	1000	−15
10	1000	1000	6	10 000	−15	2000	−21	1000	−15
11	1000	4000	3	10 000	−15	5000	−18	1000	−15
12	1000	4000	6	10 000	−15	5000	−21	1000	−15
13	4000	100	3	10 000	−15	4100	−18	4000	−15
14	4000	100	6	10 000	−15	4100	−21	4000	−15
15	4000	1000	3	10 000	−15	5000	−18	4000	−15
16	4000	1000	6	10 000	−15	5000	−21	4000	−15
17	4000	4000	3	10 000	−15	8000	−18	4000	−15
18	4000	4000	6	10 000	−15	8000	−21	4000	−15

single-step 'baseline' input function assumes that the $\delta^{18}O$ and $\delta^{2}H$ of precipitation were constant throughout the Holocene, in spite of ample evidence for climatic fluctuations that probably also affected the isotopic composition of precipitation. These include the Hypsithermal (*c.* 8000–4000 ^{14}C yr BP) and Medieval Warm Period (MWP, *c.* AD 1100–1300), during which average conditions were appreciably warmer than at present, and the Little Ice Age (LIA, *c.* AD 1450–1850), characterized by greater variability and generally lower temperatures (e.g. see Vance *et al.*, 1995; Dean *et al.*, 1996; Laird *et al.*, 1996). Reconstructed $\delta^{18}O$ records of precipitation for southwestern Ontario and central Canada, for example, include fluctuations of up to 4‰ over the course of the Holocene (Edwards *et al.*, 1996).

Nevertheless, this baseline isotopic input function has been used as a first approximation of the history of the isotopic composition of precipitation in simulations of the distribution of $\delta^{18}O$ used to constrain estimates of hydraulic conductivity (Remenda *et al.*, 1996) and average linear groundwater velocity (Desaulniers, 1986; Simpkins and Bradbury, 1992), as well as in efforts to estimate the timing of deglaciation (Hussain, 1996) and original porewater isotopic composition (Rumpf, 1996). In these studies, profiles of the distribution of $\delta^{18}O$ were simulated using the baseline isotopic input function and boundary conditions and transport parameters representative of the deposit in the advection–dispersion equation. The parameter to be constrained, the hydraulic conductivity, velocity, boundary conditions or time since deglaciation can then be altered in the simulations, thereby generating different diffusion profiles until the simulated profile matches the measured vertical profile of $\delta^{18}O$. The input function is often assumed to be a known parameter and is approximated using the baseline function described above so that other unknowns can be determined using this curve-fitting method.

In addition to consideration of the $\delta^{18}O$ and $\delta^{2}H$ signals, we also evaluate the conservativeness of the derived *d*-excess parameter ($d = \delta^{2}H - 8\delta^{18}O$). The *d* value of precipitation is determined primarily by the relative humidity, temperature and wind speed at the original vapour source, and is influenced secondarily by factors such as mixing with recycled vapour along the transport trajectory (Gat *et al.*, 1994). It is often a useful guide for identifying the source area of precipitation or changing conditions at the source area in precipitation archives (Rozanski *et al.*, 1997) because it is not strongly affected by rainout processes. However, interpretation of *d* values in existing data is complicated by the relatively large uncertainties arising because of the need to combine both $\delta^{18}O$ and $\delta^{2}H$ measurements having uncertainties in the ranges of $\pm 0{\cdot}1$ to 0·2‰ and ± 1 to 3‰ respectively.

The vertical distribution of $\delta^{18}O$ and $\delta^{2}H$ were simulated using an analytical solution of the advection–dispersion equation assuming zero velocity. Variations in the isotope content of precipitation over the Holocene were simulated by adding hypothetical 'events' to the baseline input function (Figure 1b). A more realistic Holocene input function that included the Hypsithermal, MWP and LIA was also used to generate $\delta^{18}O$ and $\delta^{2}H$ profiles.

CONCEPTUAL MODEL AND INPUT PARAMETERS

The conceptual model and input parameters used in the simulations were selected to be representative of a site within the Lake Agassiz deposit with optimal conditions for preservation of connate water: a thick, unfractured, sequence of clay, with a small hydraulic gradient. Measurements of hydraulic gradients, hydraulic conductivities and profiles of $\delta^{18}O$, $\delta^{2}H$ and major ions at two sites in Lake Agassiz deposits show that such settings do exist (Remenda, 1993; Remenda *et al.*, 1994). Field observations in previous studies have shown that the groundwater flow regime in these glaciolacustrine clay deposits consists of a weathered zone, where horizontal flow dominates, and an unweathered zone, where transport is vertical and primarily by diffusion (Figure 2) (Remenda, 1993). The water table is generally shallow (within 2 m of the ground surface) and not subject to large seasonal fluctuations (Remenda, 1993). For the purpose of this paper, the weathered zone refers to the region between the water table and the interface between the weathered and unweathered zones.

Transport of both $^{1}H_2{}^{18}O$ and $^{1}H^{2}H^{16}O$ were simulated using an analytical solution (Neville, 1996) of the one-dimensional form of the advection–dispersion equation

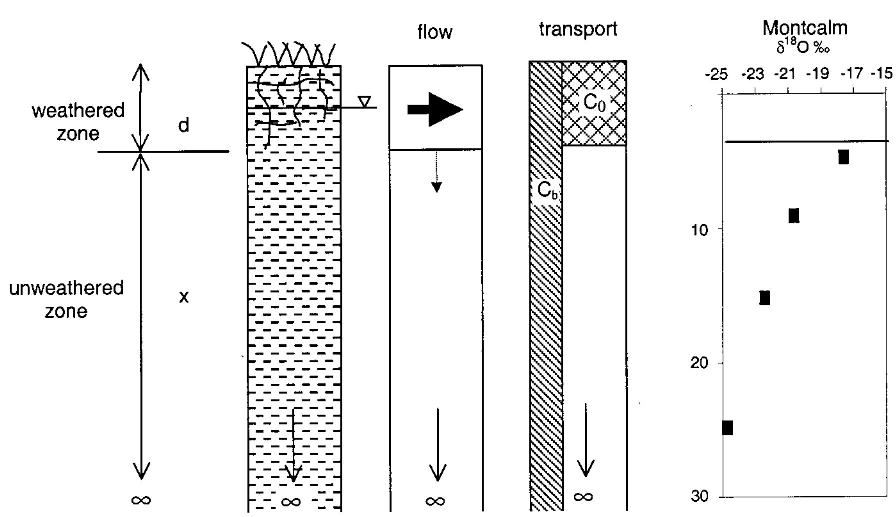

Figure 2. Conceptual model of stratigraphy, flow and transport in a thick Lake Agassiz deposit. The vertical distribution of $\delta^{18}O$ with depth is shown for the Montcalm site located in the southern part of the Lake Agassiz basin 50 km south of Winnipeg (Remenda *et al.*, 1994). At this site the vertical distribution of $\delta^{18}O$ and major ions in the unweathered zone are best approximated using a velocity of zero, suggesting that there is no vertical flow and that transport is by diffusion

$$\frac{\partial C}{\partial t} = -v\frac{\partial C}{\partial x} + D_L\frac{\partial^2 C}{\partial x^2} \tag{1}$$

with the boundary conditions:

$$C(x,0) = C_b$$
$$C(x,0,t) = C_0(t)$$
$$C(\infty,t) = C_b$$

where D_L is the hydrodynamic dispersion coefficient; C is the tracer concentration; x is the distance along the travel path; v is the average linear groundwater velocity and t is the time since the change from glacial to modern isotope contents in the weathered zone. When $v = 0$ the mechanical dispersion is negligible and $D_L = \alpha v + D^*$ simplifies to $D_L = D^*$, where α is the diffusivity and D^* is the effective diffusion coefficient. The conceptual model used here has an inflow boundary with time-varying concentration ($C_0(t)$, Type 1 inflow boundary condition), a semi-infinite domain, and uniform initial conditions (Figure 2). The parameters used for the simulations are given in Table II and are discussed below.

The weathered zone is treated as a well-mixed, step-function-type source reservoir with a concentration (C_0) that is a function of time (Figure 1b). Table I lists the values of C_0 for δ^{18}O used in the input functions. For simplicity corresponding values of C_0 for δ^2H were calculated so that all input concentrations have a common d-value of 10‰ and plot on the Global Meteoric Water Line (GMWL $\delta^2\mathrm{H} = 8\delta^{18}\mathrm{O} + 10$).

The isotopic composition of groundwater in the weathered zone is often a good approximation of the mean annual isotopic composition of local precipitation but may be complicated by preferential seasonal recharge or soilwater evaporation (Fritz *et al.*, 1987). In the baseline input function $C_0 = -15$‰ (for δ^{18}O) was used based on the isotopic composition of modern precipitation and shallow groundwater in southern Manitoba (Fritz *et al.*, 1987). Changes in C_0 over time represent changes in the mean annual isotopic composition of precipitation.

In the unweathered zone the initial porewater concentrations (C_b) represent the water present during deposition. The isotopic composition of Lake Agassiz at the time of deposition is a spatial and temporal average of late-glacial precipitation (Remenda *et al.*, 1994). Values of -25‰ for δ^{18}O and -190‰ for δ^2H were used for C_b based on the most negative values measured in Lake Agassiz deposits and contemporaneous glacial deposits in Ontario and Saskatchewan (Remenda *et al.*, 1994). Lake Agassiz sediments were deposited between about 11 700 ^{14}C years BP and 9500 ^{14}C years BP in southern Manitoba (Fenton *et al.*, 1983). This rapid deposition suggests that the assumption of a uniform initial porewater composition, a constant C_b with depth, should be valid.

A semi-infinite domain was used so only diffusion across the upper boundary was considered. Although Lake Agassiz deposits range in thickness from about 10 to 80 m, these simulations assume a thick sequence

Table II. Transport parameters used in the simulations

Parameter	Value	Source
Input concentration, $C_0(t)$	$\delta^{18}\mathrm{O} = -25^1$ to -15^2‰	[1]Remenda *et al.* (1993), [2]Fritz *et al.* (1987)
	$\delta^2\mathrm{H} = -190$ to -110‰	Calculated from δ^{18}O to plot on GMWL
Background concentration	$\delta^{18}\mathrm{O} = -25$‰	
C_B	$\delta^2\mathrm{H} = -190$‰	Remenda *et al.* (1994)
Time	10 000 years	
Velocity	0	
Effective diffusion	D^* ($^1\mathrm{H}^2\mathrm{H}^{16}\mathrm{O}$) $1{\cdot}97 \times 10^{-10}$ m^2/s	
Coefficient	D^* ($^1\mathrm{H}_2{}^{18}\mathrm{O}$) $1{\cdot}74 \times 10^{-10}$ m^2/s	Kolrud (1996)

where hydraulic gradients are low, thus porewater in the mid-section of the deposit is a sufficient distance from the upper and lower boundaries to preserve the original composition. However, where deposits are thin, diffusive overprinting from above may intersect the diffusive overprinting from below, resulting in loss of the original porewater composition.

The timing of the change from glacial to modern isotope contents (t_1) coincides with deglaciation for till deposits and lake drainage for glaciolacustrine deposits. The large glacial–interglacial change in the isotopic composition of water in the weathered zone would have occurred when Lake Agassiz drained in southern Manitoba, about 9500 ^{14}C years BP (Fenton *et al.*, 1983). Converting to calendar years gives a timing of about 10 600 calendar years BP (Stuiver and Reimer, 1993). For simplicity, the time was approximated in the simulations as 10 000 calendar years BP. All timing and age references referred to here and used in the modelling are in calendar years unless noted otherwise.

The transport of both $^{1}H_2{}^{18}O$ and $^{1}H^{2}H^{16}O$ was simulated for each of the input functions. Simulations of the vertical distribution of both δ^2H and $\delta^{18}O$ were then used to generate the equivalent *d*-excess profile. Values of δ^2H and $\delta^{18}O$ were extracted for each 5-cm interval from the two resulting vertical distribution profiles and used to calculate a *d*-excess value for that depth interval.

All source input functions began with the baseline, which was then altered to include periods of different timings and durations where the stable isotope content of precipitation differed from modern values by varying magnitudes (Figure 1b).

The input functions summarized in Table I were used to compare the sensitivity of vertical profiles of $\delta^{18}O$ and δ^2H to the timing, duration and magnitude of events, however, they do not correspond with what is known about Holocene climate on the Great Plains. A hypothetical Holocene input function was approximated by including events with timings, durations and magnitudes estimated for known Holocene events such as the Hypsithermal, MWP and LIA (Table III). Estimates of the magnitudes and durations of events for the Holocene input function were made using upper limits of reported values in order to give a best-case scenario in terms of preservation potential and a worse-case scenario for the implications to curve-fitting parameter estimation.

The $\delta^{18}O$–temperature coefficients for the mid- and high latitudes determined from the IAEA/WMO database have a range of 0·5 to 0·9‰/°C (Rozanski *et al.*, 1997). The Hypsithermal estimated at 8000 to 4000 years BP is the most prominent feature of the Holocene climate. Temperatures are estimated to have been 2 °C warmer during this period (Dean *et al.*, 1996), however, shifts of up to 4‰ have been found in inferred precipitation records for southwestern Ontario and central Canada (Edwards *et al.*, 1996). The MWP is estimated to have been 0·5–1·0 °C warmer than present and the LIA is estimated to have been 0·5–1·0 °C cooler than present. These events were approximated with 2‰ shifts in $\delta^{18}O$ using a generous $\delta^{18}O$–temperature coefficient of 2‰/°C (Table IV).

Effective diffusion coefficients of $D^* = 1{\cdot}74 \times 10^{-10}$ m^2/s for $^{1}H_2{}^{18}O$ and $D^* = 1{\cdot}97 \times 10^{-10}$ m^2/s for

Table III. Ranges for reported Holocene temperature variations

Event	Timing (years BP)	Duration (years)	Magnitude isotopes	Magnitude climate	Reference
Little Ice Age	147	420		Colder	Laird *et al.* (1996)
Medieval Warm Period	697	300		Warmer	Laird *et al.* (1996)
Hypsithermal Great Plains	4000	4000		+1–2 °C	Dean *et al.* (1996)
	4000	4000		More arid, warmer, drier	Vance *et al.* (1993)
Draining of Lake Agassiz in response to interglacial conditions	9500 ^{14}C years BP				Fenton *et al.* (1983)
			+10		Remenda *et al.* (1994)

Table IV. Summary of the timing, duration and magnitude of events included in the Holocene scenario

Event	Timing (cal. years BP)	Duration (years)	Magnitude isotopic shift ($\delta^{18}O$‰)
Little Ice Age	100	500	-2
Medieval Warm Period	600	300	$+2$
Hypsithermal	4000	4000	$+4$
Draining of Lake Agassiz in response to interglacial conditions	10 000		$+10$

$^1H^2H^{16}O$ were used in the simulations based on measurements made by Kolrud (1996) using the radial diffusion cell method on intact core samples of Lake Agassiz clay. The radial diffusion cell method, developed by Novakowski and van der Kamp (1996), is based on diffusive exchange between a cylindrical sample of clay and a fluid-filled reservoir. Similar values for the effective diffusion coefficient of $^1H_2{}^{18}O$ for the same deposit were obtained by Remenda *et al.* (1996) using column experiments ($D^* = 1{\cdot}7 \times 10^{-10}$ m^2/s).

RESULTS OF SIMULATIONS

Presented in Figure 3 are the simulated vertical profiles of $\delta^{18}O$ versus depth for the three simulations consisting of a 6‰ shift in the $\delta^{18}O$ of precipitation lasting 1000 years occurring 100, 1000 and 4000 years BP (simulations 4, 10 and 16 from Table I) presented with the baseline distribution. The distribution of $\delta^{18}O$ resulting from the 6‰ shift occurring 4000 years BP is almost identical to the baseline distribution. As can be seen in Figure 3, the profiles simulated with variations in the timing of the event differ in the top 5 m, with a maximum spread of 3‰ in $\delta^{18}O$.

Presented in Figure 4 are the simulated vertical profiles of $\delta^{18}O$ versus depth for the three simulations consisting of a 6‰ shift in the $\delta^{18}O$ of precipitation occurring 1000 years BP and lasting 100, 1000 and 4000 years (simulations 8, 10 and 12 from Table I) with the baseline distribution. The profiles simulated with variations in the duration of the event differ between about 2 and 20 m below the weathered zone, with a maximum spread of 2‰ in $\delta^{18}O$.

Presented in Figure 5 are the simulated vertical profiles of $\delta^{18}O$ versus depth for the two simulations consisting of 3 and 6‰ shifts in the $\delta^{18}O$ of precipitation lasting 1000 years and occurring 1000 years BP (simulations 9 and 10 from Table I). The profiles simulated with variations in the magnitude of the event differ between 2 and 13 m below the weathered zone with a maximum spread of 1·5‰ in $\delta^{18}O$.

The simulated vertical profiles of $\delta^{18}O$ versus depth for all of the combinations of duration and magnitude for shifts in $\delta^{18}O$ occurring 100 years BP (simulations 1–6 from Table I) are presented in Figure 6a. Differences between simulations are confined to the top 10 m below the weathered zone and have a maximum spread of 5‰ in $\delta^{18}O$.

The simulated vertical profiles of $\delta^{18}O$ versus depth for all of the combinations of duration and magnitude for shifts in $\delta^{18}O$ occurring 1000 years BP are presented in Figure 6b (simulations 7–12 from Table I). Differences between simulations are confined to the top 13 m below the weathered zone and have a maximum difference in $\delta^{18}O$ of 2‰.

Simulations of transport for all of the combinations of duration and magnitude for shifts in $\delta^{18}O$ occurring 4000 years BP are presented in Figure 6c (simulations 13–18 from Table I). Differences between simulations are confined to the top 15 m below the weathered zone and have a maximum difference in $\delta^{18}O$ of 1‰.

All of the simulations presented in the Figures here are of $\delta^{18}O$. The profiles of δ^2H differ from the baseline at approximately the same depths but the magnitude of the offsets are scaled to the wider range of values in the input function (C_0 ranged from -110 to -190‰ for δ^2H versus -15 to 25‰ for $\delta^{18}O$).

All of the input functions used in the simulations presented in the sensitivity analysis included events

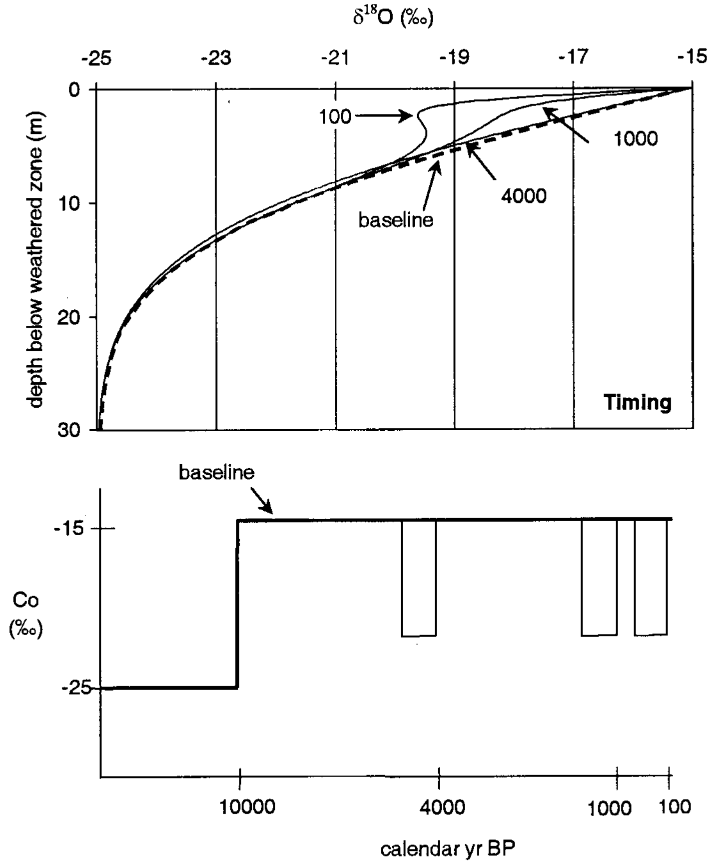

Figure 3. The vertical distribution of $\delta^{18}O$ with depth below the active zone using an input function where only the timing of a 6‰ change in $\delta^{18}O$, with a duration of 1000 years is varied (the timing of the events were 100 years BP, 1000 years BP, and 4000 years BP, corresponding to simulations 4, 10 and 16, respectively, from Table I)

where the isotopic composition of Holocene precipitation was more negative than modern, as would be expected during colder climate periods. Warm climate events, consisting of a positive shift from the baseline function, have the same sensitivity as the negative shifts but result in distributions that are mirrored across the baseline function.

The Holocene input function results in a vertical distribution of $\delta^{18}O$ that differs from the baseline by about 0·6‰ in $\delta^{18}O$ (Figure 7). The equivalent $\delta^{2}H$ distribution varies by about 5‰.

The initial porewater and all the input function waters had a *d*-excess of 10‰. The different rates of transport of $^{1}H_2{}^{18}O$ and $^{1}H^{2}H^{16}O$ due to differences in their effective diffusion coefficients result in simulated *d*-excess values of up to 13‰ (Figure 8). Although the absolute values of *d*-excess from limited data available from the Montcalm site (Figure 8) are somewhat lower, the trend is consistent with simulated *d*-excess profiles.

DISCUSSION

Changes in the isotopic composition of water in the source zone are propagated downward by diffusion of $^{1}H_2{}^{18}O^{1}$ and $H^{2}H^{16}O$ in the porewaters of the underlying unweathered zone in thick, unfractured clay aquitards. The sensitivity of the resulting isotopic profile to these changes determines the nature of the

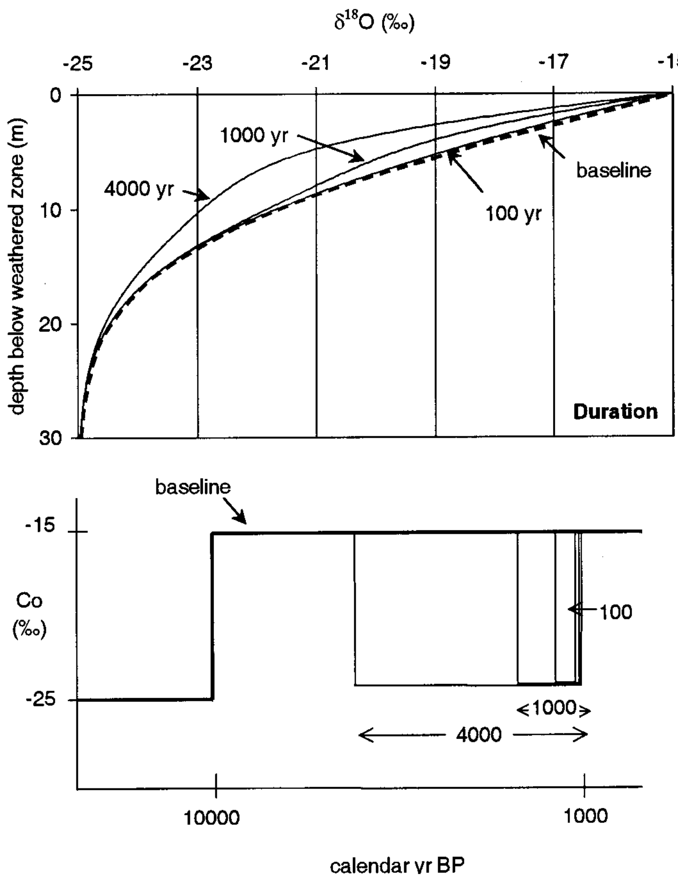

Figure 4. The vertical distribution of $\delta^{18}O$ with depth below the active zone using an input function where only the duration of a 6‰ change in $\delta^{18}O$, occurring 1000 years BP is varied (the duration of the events were 100 years and 4000 years corresponding to simulations 8, 10 and 12, respectively, from Table I)

palaeoprecipitation record preserved in aquitards and has implications for the estimation of hydrogeological parameters.

The most obvious result of this study is the importance of the timing of Holocene events to their preservation. This is illustrated by comparing the impact of events of the same duration and magnitude that differ in timing (Figure 6). Recent events are preserved as large, distinct offsets from the baseline isotopic distribution, whereas more distance events are greatly subdued. Recent climate shifts are preserved at shallow depths, an area where signals are vulnerable owing to the potential for infiltration of modern precipitation through desiccation fractures, fluctuations in the water table and agricultural activity. The profiles in the deep groundwater zone are less vulnerable to disturbance from surface processes but contain earlier, more smoothed signals that are preserved as slight alterations in the overall shape of the diffusion profile.

The importance of the timing of events is evident in the isotopic profiles generated using the Holocene input function. The effects of the LIA and MWP are visible in the top few metres of the isotopic profiles generated using the Holocene input function. The subdued nature of the signal preserved for these two very recent events is in part related to the opposite directions of the isotopic shifts associated with the MWP and LIA events. In effect, the depleted isotopic composition of the most recent event (LIA) compensates for the enriched composition of the MWP. The effect of the Hypsithermal in the Holocene simulations is found in the positive offset of about 0·6‰ in $\delta^{18}O$ (about 5‰ in $\delta^{2}H$) from the baseline profile. Although fairly small,

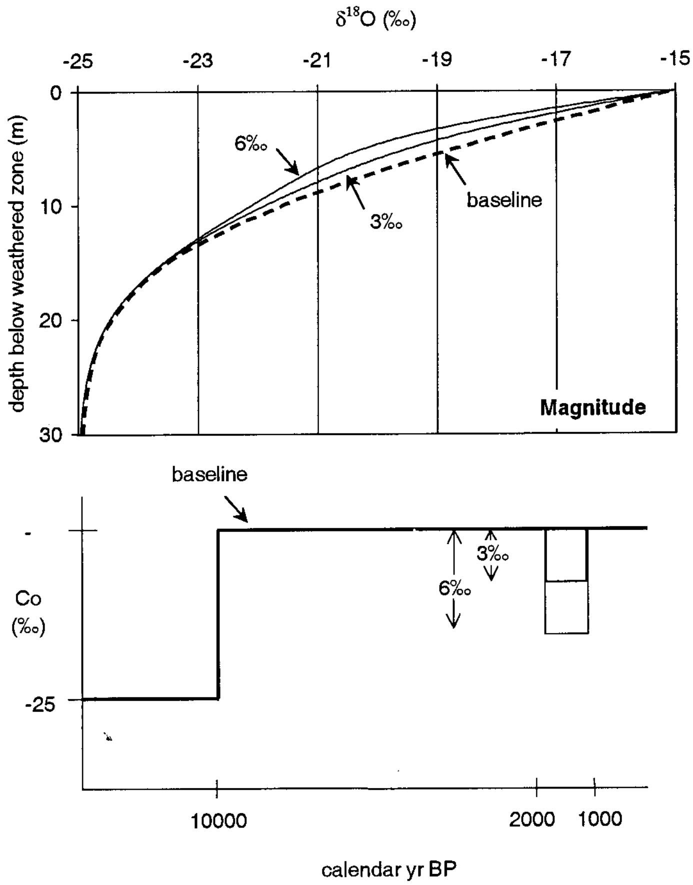

Figure 5. The vertical distribution of $\delta^{18}O$ with depth below the active zone using an input function where only the magnitude of 1000 years duration events occurring 1000 years BP are varied (the magnitude of the events were 3‰ and 6‰, corresponding to simulations 9 and 10, respectively, from Table I)

the preservation of this signal is encouraging in that it shows that the effects of mid-Holocene events are not lost in the archive.

The *d*-excess parameter is not conservative in a groundwater system where the dominant mode of transport is diffusion. However, the positive shift in *d*-excess is predictable and consequently can be taken into consideration when interpreting *d*-excess data. The *d*-excess may provide another means of identifying changes in the isotopic composition of water in the weathered zone. Where concentration gradients are large, transport fluxes are high and the differences in the effective diffusion coefficients will have the greatest effect, resulting in an increase in the *d*-excess. In the baseline scenario all of the source zone waters were held to a *d*-excess of 10. However, when *d*-excess values are calculated from the simulated profiles, an additional *d*-excess of $\approx$3‰ is created (Figure 8). This additional *d*-excess is a measure of the difference between the vertical distributions of $^1H^2H^{16}O$ and $^1H_2{}^{18}O$ arising because of their differing diffusion coefficients.

The vertical distribution of *d*-excess for scenarios that include hypothetical events during the Holocene (Figure 8, e.g. simulation of 10–1000 years BP, 1000 years duration, 6‰ shift in $\delta^{18}O$; and simulation 12–1000 years BP, 4000 years duration, 6‰ shift in $\delta^{18}O$) preserve evidence of distinct events (Figure 8) that are not found in the individual profiles of $\delta^{18}O$ and δ^2H (Figure 6b). The two distinctive peaks in the *d*-excess profile for simulations 10 and 12 correspond to two areas of the diffusion profiles where the concentration gradients are higher, reflected in slightly different slopes in the profile. If the vertical distribution of *d*-excess

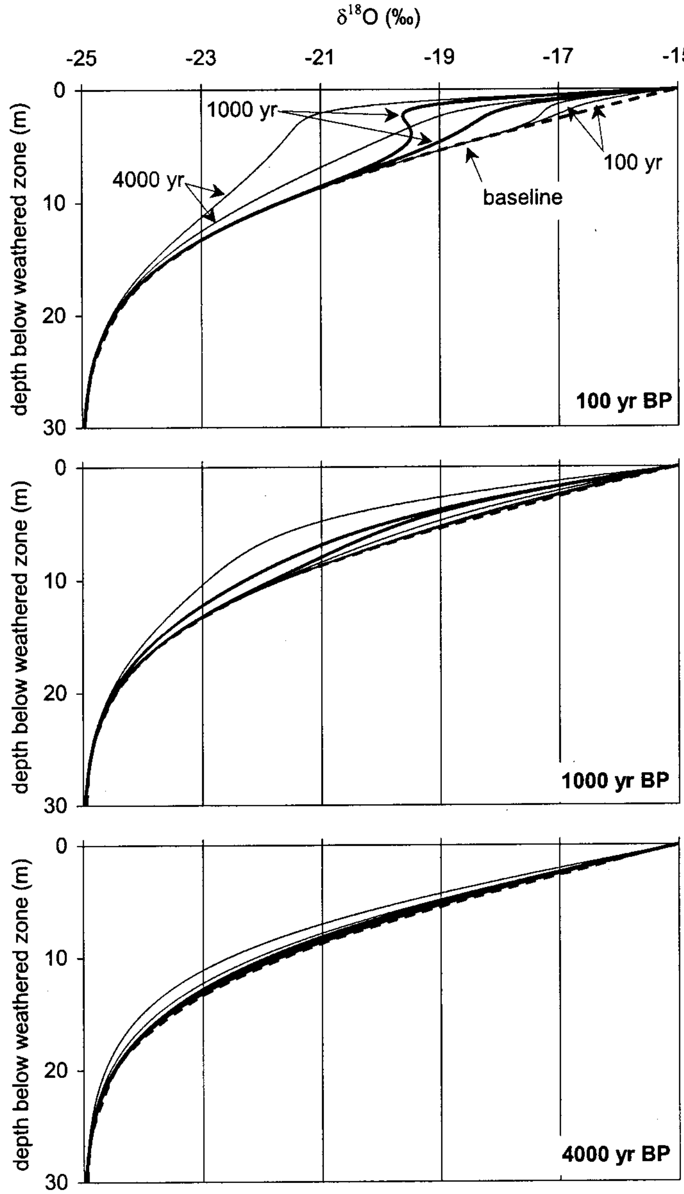

Figure 6. (a) All combinations of duration and magnitude for changes in $\delta^{18}O$ occurring 100 years BP (simulations 1–6 from Table I). The simulations predict the distribution of δ^2H and $\delta^{18}O$ in the unweathered zone, so all depths refer to depth below the weathered zone. (b) All combinations of duration and magnitude for changes in $\delta^{18}O$ occurring 1000 years BP (simulations 7–12 from Table I). (c) All combinations of duration and magnitude for changes in $\delta^{18}O$ occurring 4000 years BP (simulations 13–18)

is examined for a scenario occurring 4000 years BP (Figure 8, e.g. simulation 16–4000 years BP, 1000 years duration, 6‰ shift in $\delta^{18}O$; and simulation 18–4000 years BP, 4000 years duration, 6‰ shift in $\delta^{18}O$) individual events are no longer visible. The *d*-excess parameter may extend the preservation of fluctuations in the isotopic composition of precipitation in porewater.

The shift in *d*-excess of about 3‰ in the Montcalm profile could simply reflect diffusional effects, rather than a change in source-water *d*-excess. The offset between the Montcalm data and the simulations is due

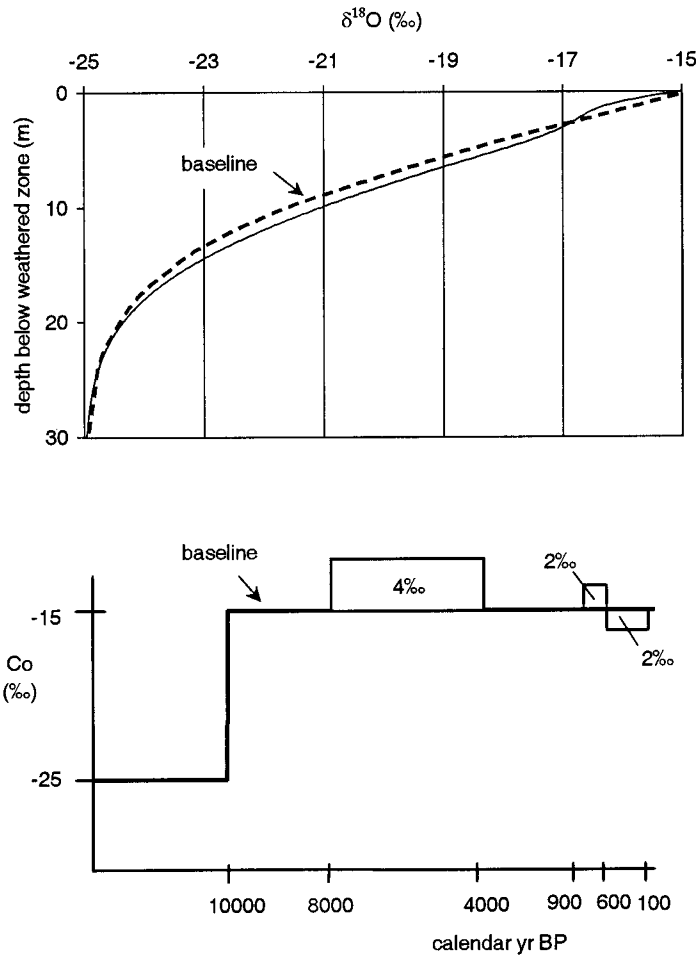

Figure 7. The vertical distribution of $\delta^{18}O$ with depth below the active zone using an input function consisting of shifts in $\delta^{18}O$ estimated for the Holocene summarized in Table IV

to the use of 10‰ for *d*-excess of recharge waters in the simulations, whereas shallow groundwaters in southern Manitoba have *d*-excess in the range of 0 to 5‰ (Fritz *et al.*, 1987).

The isotopic distributions simulated using the Holocene input function also can be used to evaluate the implications of using the baseline input function to estimate hydrogeological parameters. Although recent events, such as the MWP and LIA, have a good preservation potential, they likely have little effect on parameters derived from fitting curves to isotopic profiles because they affect such a short portion of the overall curve (first few metres) and because they are located directly below the weathered zone, where any offsets are usually attributed to influence of the weathered zone.

The long duration of the simulated Hypsithermal creates a measurable offset from the baseline isotopic distribution over a large part of the profile and consequently has the potential to have a greater impact on parameter estimation than more recent events. The magnitude of the offset will vary with the timing, duration and magnitude of the Hypsithermal, which may vary from site to site, but will always result in a positive offset from the baseline isotopic distribution. To achieve an equivalent positive offset using the baseline input function one would have to increase the velocity or assume that deglaciation occurred earlier. In other

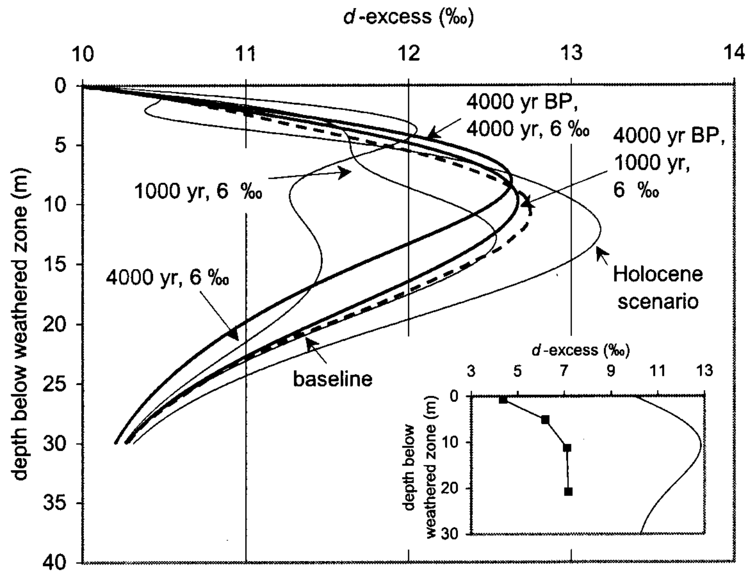

Figure 8. Distribution of *d*-excess with depth below the weathered zone for the baseline scenario, the estimated Holocene scenario, and simulations 10, 12, 16 and 18 (Table I). Inset shows *d*-excess measured at the Montcalm site (Remenda, 1993) with the baseline simulation

words, exclusion of the Hypsithermal could result in overestimation of the advective component or time since deglaciation.

Quantitatively evaluating the magnitude of the overestimation is specific to the transport parameters and boundary conditions used for each site. The scenario presented here suggests Holocene climate fluctuations would have a minimal effect on the hydrogeological parameters estimated from fitting simulated curves to isotopic profiles as long as the parameters are estimated using a 0·6‰ envelope around the best fit profile of $\delta^{18}O$ (5‰ for δ^2H), the magnitude of the positive overestimation of the advective component using these offsets is likely not significant considering the ranges of uncertainty commonly used when fitting hydrogeological parameters. The fact that it is an overestimation is important in that it further supports the notion that in many aquitards diffusional transport dominates, as suggested by isotopic evidence.

CONCLUSIONS

Recent events clearly have the greatest chance of being preserved as prominent deviations in the vertical distribution of $^1H_2{}^{18}O$ and $^1H^2H^{16}O$ in aquitard porewater from the baseline isotope profile. Events in the mid-Holocene (those ending 4000 years BP) of sufficient magnitude and duration are preserved as systematic, although subdued, offsets from the baseline profiles. Nevertheless, the isotopic composition of porewater in aquitards can be used to add to our knowledge of Holocene climate variations by providing a means to reconstruct or constrain $\delta^{18}O$ and δ^2H of palaeoprecipitation, particularly for the mid- to late Holocene. The palaeoprecipitation record preserved in aquitards where transport is by diffusion is similar to the palaeotemperature record preserved in the temperature distribution in boreholes. This suggests that the same techniques (such as Monte Carlo inversion, Dahl-Jensen *et al.*, 1998) that have been used to obtain a temperature history from temperature profiles measured in boreholes also could be used to obtain a time-series of the isotopic composition of precipitation from isotopic profiles in aquitards.

The range of possible input functions that generate similar and reasonable diffusion profiles emphasizes that solutions are non-unique. In order to maximize the resolution of a palaeoprecipitation history obtained from the inversion of isotopic profiles in clay aquitards, all other parameters that also affect the isotopic distribution — hydraulic conductivity, velocity and effective diffusion coefficients — must be well characterized for each site. The stacking of isotopic profiles from multiple cores from the same aquitard subject to the same source function should also help constrain the recovered palaeoprecipitation history.

In addition, the *d*-excess may enhance the Holocene palaeoprecipitation record preserved in the diffusive environment of a glaciolacustrine deposit by amplifying changes in the shape of the diffusion profile not easily identifiable in the individual profiles of $\delta^{18}O$ or $\delta^{2}H$.

Short-term fluctuations in the isotopic composition of precipitation over the Holocene would have little effect on the estimation of hydrogeological parameters. Long-duration events such as the Hypsithermal can create isotope profiles that mimic profiles generated using slightly larger advective components or longer times since deglaciation. This is likely not significant in most applications given the ranges of uncertainty commonly used when fitting hydrogeological parameters.

ACKNOWLEDGEMENTS

This manuscript benefited from the comments of B. Wolfe and two anonymous reviewers. This work was supported in part by NSERC PGS-B to SJB and NSERC grants to TWD and VHR.

REFERENCES

Dahl-Jensen D, Mosegaard K, Gundestrup N, Clow GD, Johnsen SJ, Hansen QW, Balling N. 1998. Past temperatures directly from the Greenland ice sheet. *Science* **282**: 268–271.

Dean WE, Ahlbrandt TS, Anderson RY, Bradbury JP. 1996. Regional aridity in North America during the middle Holocene. *The Holocene* **6**: 145–155.

Desaulniers DE. 1986. *Groundwater origin, geochemistry and solute transport in three major glacial clay plains of east-central North America*. PhD thesis, University of Waterloo: Waterloo, Canada.

Edwards TWD, Wolfe BB, MacDonald GM. 1996. Influence of changing atmospheric circulation on precipitation $\delta^{18}O$ — temperature relations in Canada during the Holocene. *Quaternary Research* **46**: 211–218.

Fenton MM, Moran SK, Teller JT, Clayton L. 1983. Quaternary stratigraphy and history in the southern part of the Lake Agassiz Basin. *Glacial Lake Agassiz*, Teller JT, Clayton L (eds). *Geological Association of Canada Special Paper* **26**: 949–974.

Fritz P, Drimmie RJ, Frape SK, O'Shea K. 1987. The isotopic composition of precipitation and groundwater in Canada. *IAEA-SM-299/17* International Atomic Energy Agency: Vienna.

Gat JR, Bowser CJ, Kendall C. 1994. The contribution of evaporation from the Great Lakes to the continental atmosphere: estimate based on stable isotope data. *Geophysical Research Letters* **21**: 557–560.

GRIP members. 1993. Climate instability during the last interglacial period recorded in the GRIP ice core. *Nature* **364**: 203–207.

Grootes PM, Stuiver M, White JWC, Johnsen SJ, Jouzel J. 1993. Comparison of oxygen isotope records from the GISP2 and GRIP Greenland ice cores. *Nature* **366**: 552–554.

Hussain MM. 1996. *Origin and persistence of Pleistocene and Holocene water in a regional clayey aquitard and underlying aquifer in part of southwestern Ontario*. PhD thesis, University of Waterloo: Waterloo, Canada.

Kolrud E. 1996. *Determination of effective diffusion coefficients of ^{18}O and ^{2}H in a glaciolacustrine clay using the radial diffusion cell method*. BsC Thesis, Queen's University: Kingston, Canada.

Laird KR, Fritz SC, Grimm EC, Mueller PG. 1996. Century-scale paleoclimate reconstruction from Moon Lake, a closed-basin lake in the northern Great Plains. *Limnology and Oceanography* **41**: 890–902.

Neville CJ. 1996. *ONED. A Package of Three Analytical Solutions for One-Dimensional Solute Transport*, *Version 1*. Klohn–Crippen Consultants Ltd.: Calgary, Alberta.

Novakowski KS, van der Kamp G. 1996. The radial diffusion method 2. A semianalytical model for the determination of effective diffusion coefficients, porosity and adsorption. *Water Resources Research* **32**: 1823–1830.

Remenda VH. 1993. *Origin and migration of natural groundwater tracers in thick clay tills of Saskatchewan and the Lake Agassiz clay plain*. PhD Thesis, University of Waterloo: Waterloo, Canada.

Remenda VH, Cherry JA, Edwards TDW. 1994. Isotopic composition of old ground water from Lake Agassiz: implications for late Pleistocene climate. *Science* **266**: 1975–1987.

Remenda VH, van der Kamp G, Cherry JA. 1996. Use of vertical profiles of ^{18}O to constrain estimates of hydraulic conductivity in a thick, unfractured aquitard. *Water Resources Research* **32**: 2979–2987.

Rozanski K, Johnsen SJ, Schotterer U, Thompson LG. 1997. Reconstruction of past climates from stable isotope records of palaeo-precipitation preserved in continental archives. *Hydrological Sciences — Journal des Sciences Hydrologiques* **142**: 725–745.

Rumpf KH. 1996. The physical and chemical hydrogeology of the Little Clay Belt, District of Timiskaming. MSc Thesis, University of Waterloo: Waterloo, Canada.

Simpkins WW, Bradbury KR. 1992. Groundwater flow, velocity, and age in a thick, fine-grained unit in southeastern Wisconsin. *Journal of Hydrology* **132**: 283–319.

Stuiver M, Reimer PJ. 1993. Extended ^{14}C data base and revised CALIB 3·0 ^{14}C age calibration program. *Radiocarbon* **35**: 215–230.

Vance RE, Beaudoin AB, Luckman BH. 1995. The paleoecological record of 6 ka bp climate in the Canadian prairie provinces. *Geographie Physique et Quaternaire* **49**: 81–98.

